A Man-Portable Magnetoelectric DC Magnetic Sensor With Extremely High Sensitivity

Ying Shen, Dingyi Ma, and Junqi Gao

***Abstract*— This letter presents an advanced 3-axis portable dc magnetic sensor unit consisting of magnetoelectric (ME) composites and a custom lock-in amplifier circuit, which has extremely high sensitivity and detection resolution. The Metglas/Pb(Zr,Ti)O3 ME composites driven by a lock-in amplifier circuit exhibit a high sensitivity of 5 V/Oe. Moreover, the equivalent magnetic noise of the unit is limited to 128 pT/√Hz at 1 Hz. Therefore, a dc magnetic field as small as 1 nT can be sensed directly in the time domain. The entire 3-axis dc magnetic sensor is portable and energy-efficient, making it promising for magnetic navigation applications based on sensing variations in the magnitude and orientation of local geomagnetic fields.**

***Index Terms*— Magnetoelectric, magnetic sensor, lock-in circuit, resolution.**

I. Introduction

ANIMAL behavioral studies have provided abundant evidence for magnetic compass orientation and navigation by sensing the magnetic field gradient of the Earth. Among approximately 50 species, animals include birds [1], sea turtles [2], and sharks [3]. Though the underlying biophysical mechanisms remain elusive [4], animal capabilities have fueled considerable interest in developing sensitive magnetometers for geophysical measurements, which are often made in remote areas of the world. Sensing devices involving optically pumped magnetometers and SQUIDs operated at liquid nitrogen temperatures have the required sensitivity and are used invariably [5]. In outdoor and underwater applications, however, the inconvenience of using such energy hungry and bulky devices often outweighs the advantage of very high sensitivity; alternative instruments, such as coil magnetometers and fluxgates, are much more widely used [6]–[8]. However, a price is paid for more convenient devices operating at room temperature: the signal-to-noise ratio will inevitably degrade as the handiness is enhanced.

This situation may be about to change dramatically, however, with the advent of the giant magnetoelectric (ME) effect observed in ME heterostructure composites [9]. In the early 2000s, composites consisting of the rare-earth-iron alloy $Tb_{1-x}Dy_xFe_2$ (Terfenol-D) were theoretically and experimentally proven to have a large ME effect [10], [11]. Since then, various ME composite systems with high ME effect have been reported [10]–[17], and technological ME devices have been developed, in particular, AC and DC magnetic sensors [20]–[22]. For example, extremely low noise AC magnetic sensors were achieved with Metglas/Piezo-fibers laminates [23], [24]; in addition, thin-film ME sensors were designed and fabricated by MEMS technology for chip level integrations [25]–[28]. Furthermore, polymer-based ME composites were exploited to develop flexible magnetic sensors [29], [30].

Despite this progress, multi-axis ME DC magnetic sensors with compact size have not been well developed. For precise orientation and navigation, there has been a critical need to further improve sensitivity and detection resolution. Here, we present a 3-axis highly sensitive ME DC magnetic sensor through a combination of the giant ME effect and lock-in amplifier circuitry. The unit is optimized with low energy consumption of 300 mW, making it more practical for device applications. The sensor shows a sensitivity of 5 V/Oe and a high detection resolution of 1 nT. Such a portable magnetic sensor is promising for application in electric compasses and geomagnetic field sensing.

II. DC Magnetic Sensor Design

A photograph of the 3-axis DC magnetic sensor developed in this work is shown in Fig. 1(a). It contains three ME composite units at the top and a lock-in amplifier circuit installed in the base housing with batteries. The total size of this unit is approximately 400 cm^3. A driving inductance coil was wrapped around each ME composite unit [31], as illustrated in the insert picture of Fig. 1(a).

A. ME Composites

The laminated ME composites consisting of PZT (Applied Ceramics Inc., China, piezoelectric coefficients:

Manuscript received July 3, 2018; revised July 17, 2018; accepted July 17, 2018. Date of publication July 23, 2018; date of current version August 23, 2018. This work was supported in part by the Stable Supporting Fund of Acoustic Science and Technology Laboratory under Grant SSJSWDZC2018007 and in part by the Fundamental Research Funds for the Central Universities under Grant HEUCFG201826, Grant HEUCFP201748, and Grant HEUCFJ180508. The review of this letter was arranged by Editor E. A. Gutiérrez-D. *(Corresponding author: Junqi Gao.)*

Y. Shen is with the Acoustic Science and Technology Laboratory, Harbin Engineering University, Harbin 150001, China, also with the Key Laboratory of Marine Information Acquisition and Security (Harbin Engineering University), Ministry of Industry and Information Technology, Harbin 150001, China, also with the College of Underwater Acoustic Engineering, Harbin Engineering University, Harbin 150001, China, and also with MultiDimension Technology Co., Ltd., Zhangjiagang 215600, China.

D. Ma and J. Gao are with the Acoustic Science and Technology Laboratory, Harbin Engineering University, Harbin 150001, China, also with the Key Laboratory of Marine Information Acquisition and Security (Harbin Engineering University), Ministry of Industry and Information Technology, Harbin 150001, China, and also with the College of Underwater Acoustic Engineering, Harbin Engineering University, Harbin 150001, China (e-mail: gaojunqi@hrbeu.edu.cn).

Color versions of one or more of the figures in this letter are available online at http://ieeexplore.ieee.org.

Digital Object Identifier 10.1109/LED.2018.2858280

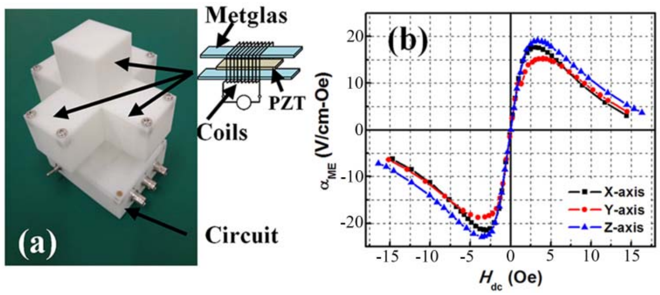

Fig. 1. (a) Schematic of the triple-axis DC magnetic sensor; (b) ME voltage coefficients for the Metglas/PZT composites. The insert is an illustration of the active mode of ME composites.

$d_{31} = -270$ pC/N, $d_{33} = 550$ pC/N) and Metglas foils 2605SA1 (Metglas Inc., US, magnetostrictive coefficient $\lambda = 27$ ppm) were fabricated in a sandwich structure. It is critical to control the process precisely in order to obtain a better ME coupling effect [32], [33]. In detail, five pieces of 200 μm thick PZT fibers were oriented along the long axis to form a piezoelectric layer that was 1 cm wide and 4 cm long. Two interdigitated (ID) Kapton®-based electrodes were then bonded to the top and bottom surfaces of the piezoelectric layer in a multi push-pull configuration by using epoxy (West System Epoxy 105/206 was mixed at mass ratio = 5:1). The assembly was then placed in a vacuum bag and subsequently evacuated. The epoxy can be cured at room temperature for 24 hours. Three Metglas foils of 10 cm in length and 1 cm in width were then laminated onto both the top and bottom surfaces of the piezoelectric layer by using the same epoxy. The ME composites were then cured at room temperature for 24 hours by using the same vacuum bag pressure method.

Fig. 1(b) shows the ME voltage coefficient α_{ME} as a function of H_{dc} for the three ME laminates. All three laminates have similar ME coefficients under a *DC* magnetic field. The α_{ME} increases linearly with increasing H_{dc} up to 3 Oe, reaching a maximum value around $\alpha_{ME} = 18$ V/cm-Oe. Please note that the ME laminates have been designed to sense the DC magnetic field; thus, the values of $\partial\alpha_{ME}/\partial H_{dc}$ are more important compared to the maximum values of α_{ME} [34]. Moreover, the induced voltage is independent of the H_{dc} history, and nearly no offset value was found near $H_{dc} = 0$ Oe. In addition, as the direction of H_{dc} is changed, the output signals change phase. Such phase shift could be potentially used to distinguish the magnetic field orientation.

B. Lock-in Circuit

A lock-in circuit was designed to contain 3 independent channels to drive inductance coils and simultaneously capture the signals from three ME composites. The total size of the circuit was 8 cm×6 cm. With respect to the circuit design, low power IC chips were employed to control the total power consumption to 300 mW, which allowed for the circuit to be powered by two 5 v batteries.

Fig. 2 shows the functional blocks of the custom-designed lock-in circuit. One of the most important parts is the analog sine wave oscillator. In this design, a Wien bridge oscillator circuit is implemented to generate the sine wave, driving

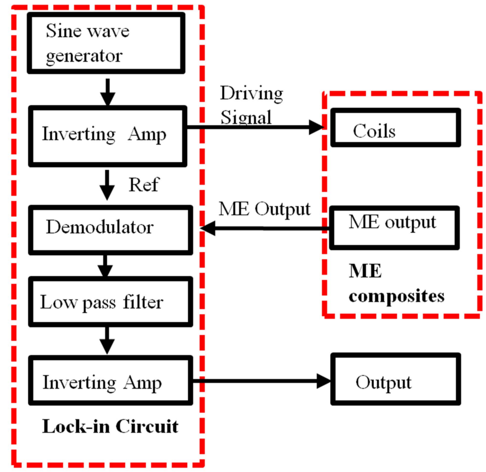

Fig. 2. Schematic layout of the lock-in circuit design.

signals at frequency of 1 kHz (off resonance frequency) using a 59 kohm resistor and a 2700 pF capacitor. The amplitude of the driving signal can be modulated by the following analog amplification circuit. Due to the nonlinear ME property, when applying AC and DC magnetic fields to the ME composites, an induced voltage is obtained [35]:

$$V_{ME}^{Nonlinear} \approx a_{ME}^{Nonlinear} \times H_{dc} \times H_{ac}\sin(2\pi f \times t + \theta_1) \quad (1)$$

where $V_{ME}^{Nonlinear}$ is the output of ME composites, $a_{ME}^{Nonlinear}$ is the nonlinear ME coefficient, H_{dc} is the DC magnetic field to be measured, H_{ac} is the AC magnetic field generated by the induction coil, f is the driving frequency at 1 kHz, and θ_1 is the phase of the driving signal.

The output signal $V_{ME}^{Nonlinear}$ was captured by the lock-in circuit and then demodulated using an AD835 multiplier with the help of a reference signal provided by the oscillator, which can be expressed as:

$$\begin{aligned} V_{signal} &= V_{ME}^{Nonlinear} \times V_{ref} = a_{ME}^{Nonlinear} \times H_{dc} \\ &\quad \times H_{ac}\sin(2\pi f \times t + \theta_1) \times A\sin(2\pi f \times t + \theta_{ref}) \\ &= \frac{1}{2} \times a_{ME}^{Nonlinear} \times H_{dc} \times H_{ac} \times A \times \cos(\theta_1 - \theta_{ref}) \\ &\quad - \frac{1}{2} a_{ME}^{Nonlinear} \times H_{dc} \times H_{ac} \\ &\quad \times A\cos(2\pi(2f) \times t + \theta_1 + \theta_{ref}) \end{aligned} \quad (2)$$

where V_{signal} is the output signal after demodulation, A is the amplitude of reference signal, and θ_{ref} is the reference signal phase. Clearly, the signal contained one DC and one 2 kHz component after demodulation. To obtain the desirable DC component, a low pass filter with cutoff frequency of 1.5 Hz was designed to reject the high-frequency parts. Thus, the relationship between the applied DC magnetic field and the output signal is $V_{out} = S \times H_{dc}$, where S is defined as the sensitivity in V/Oe.

III. Results and Discussions

A. Sensitivity and Noise

The sensitivity and noise power spectra density were first characterized. Fig. 3 (a) shows the sensitivity values for the

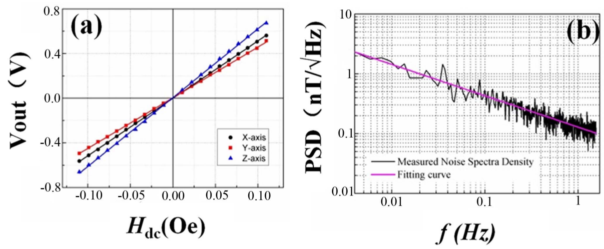

Fig. 3. (a) Sensitivity of the 3-axis DC magnetic sensor: the scatter points are experimental data, and the solid lines indicate their linear fitting results; (b) Equivalent magnetic noise of the DC magnetic sensor.

x-, y- and z-axis of the magnetometer. The scattering points refer to the measured data, and the solid lines were the linear fitting curves of the data. The magnetometer displays show the desirable linearity as a function of the external DC magnetic field in the range of −0.1 to 0.1 Oe. In particular, the sensitivity values of each orthogonal transducer unit were determined to be 5.15, 4.53 and 6.16 V/Oe. This result represents a remarkable 200 times enhancement compared to the reported Metglas/Polymer ME DC magnetic sensor [36] and a 30 times increase relative to the Metglas/PZT sensor [34]. The extremely high sensitivity is due to enhanced magnetic flux concentration effect originated with the long Metglas foils [34] and the high amplification gain of the lock-in circuit. Fig. 3(b) shows the measured magnetic noise density as well as the fitting curve modeled by employing equation $N_{\mathrm{PSD}} = N_{mag@1Hz}/f^{B}$, where N_{PSD} is the fitting noise spectrum, $N_{mag@1Hz}$ is the magnetic noise density at frequency of 1 Hz, f is the frequency, and B is the frequency index that indicates the noise attenuation rate as increasing frequency. By fitting the measured data, $N_{mag@1Hz}$ was determined to be 128 pT/$\sqrt{}$Hz, and the frequency index B was found to be 0.56, which implies that the low-frequency noise was dominated by $1/f$ noise. Based on the classic noise theory of $1/f$ noise [37], the root mean squared (RMS) noise N_{RMS} can be calculated by:

$$N_{RMS} = N_{mag@1Hz} \times \sqrt{\ln \frac{f_H}{f_L}} \tag{3}$$

where f_H and f_L refer to the up and low limit of the working frequency (taken here to be $f_{\mathrm{H}} = 1.5$ Hz and $f_{\mathrm{L}} = 1$ mHz), respectively. Based on (3), the N_{RMS} is calculated to be 0.4 nT, thereby implying a minimum 0.8 nT theoretical detection resolution of the sensor, given that the SNR is 2.

B. Resolution

The magnetic resolution of the ME DC magnetic sensor was then characterized; small DC magnetic field variations were applied along the long axis of one ME composite through the H-coils driven by a waveform generator. A small step-function voltage output of the sensor was detected with SNR=2 during measurement.

Fig. 4 shows the induced output voltages from the x-component of the sensor in response to the small magnetic field changes. The DC magnetic field variations ΔH_{dc} as small as 1 nT could be detected, which are very close to the calculated minimum detection resolution value of 0.8 nT. Note that the y and z components show similar results, which were

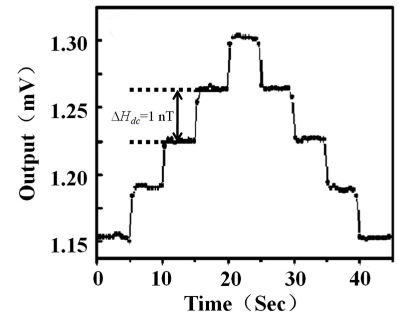

Fig. 4. Resolution of the DC magnetic sensor in response to small DC magnetic field changes. A small DC magnetic field of 1 nT is applied by the H-coils.

TABLE I
COMPARISON WITH OTHER RELATED SENSORS

Technology	Package	Sensitivity (V/G)	Resolution (nT)	Ref
Hall sensor (AKM EQ-430L)	Standalone	-	15000	Datasheet
TMR(NXP MAG3110)	Standalone	-	250	Datasheet
AMR(MEMSIC MMC 5883MA)	Standalone	-	40	Datasheet
Microfluxgate(TI DRV425)	Standalone	-	17	Datasheet
ME(Metglas/FeNi/ PZT-5A)	Test Bench	-	7	Ref[39]
ME(Merglas/PZT)	Test Bench	0.17	5	Ref[34]
Polymer ME(Metglas/PVDF)	Standalone	1.5	70	Ref[40]
ME(Merglas/PZT)	Standalone	5	1	This work

not illustrated here. This is a 6 times greater field detection ability than the previously reported ME DC sensors [34]. Due to the identical increase and decrease in change manners, the sensor also exhibits great repeatability and no hysteresis.

As shown in Table I, the proposed sensor shows excellent sensitivity and resolution compared to ME-based magnetic sensors and other MEMS sensors. Although some ultralow noise fluxgate magnetometers have lower noise floor [38], such as MAG-03 (Bartington), TFM100 (Billinsley), the 1 nT effective detection resolution poses such ME DC magnetic sensors as viable competitors for opportunities in low cost and sensitive vector magnetometers.

IV. CONCLUSION

In summary, an advanced 3-axis ME DC magnetic sensor has been developed, which has compact size and low power consumption. The sensitivity of the magnetic sensor can reach as high as 5 V/Oe, and the noise density is measured to be 128 pT/rtHz at 1 Hz. The sensor has effective detection resolution of $\Delta H_{\mathrm{dc}} = 1$ nT, which is a direct consequence of its merit of high sensitivity and the low self-noise. Such ME DC magnetic sensor is an excellent candidate for sensors with high sensitivity and resolution for weak magnetic field detection applications.

REFERENCES

[1] K. Maeda, K. B. Henbest, F. Cintolesi, I. Kuprov, C. T. Rodgers, P. A. Liddell, D. Gust, C. R. Timmel, and P. J. Hore, “Chemical compass model of avian magnetoreception,” *Nature*, vol. 453, pp. 387–390, May 2008, doi: 10.1038/nature06834.

[2] K. J. Lohmann, S. D. Cain, S. A. Dodge, and C. M. F. Lohmann, "Regional magnetic fields as navigational markers for sea turtles," *Science*, vol. 294, no. 5541, pp. 364–366, 2001, doi: 10.1126/science.1064557.

[3] C. G. Meyer, K. N. Holland, and Y. P. Papastamatiou, "Sharks can detect changes in the geomagnetic field," *J. Roy. Soc. Interface*, vol. 2, no. 2, pp. 129–130, 2005, doi: 10.1098/rsif.2004.0021.

[4] K. J. Lohmann, "Q&A: Animal behaviour: Magnetic-field perception," *Nature*, vol. 464, pp. 1140–1142, Apr. 2010, doi: 10.1038/4641140a.

[5] H. J. Barthelmess, M. Halverscheid, B. Schiefenhovel, E. Heim, M. Schilling, and R. Zimmermann, "Low-noise biomagnetic measurements with a multichannel DC-SQUID system at 77 K," *IEEE Trans. Appl. Supercond.*, vol. 11, no. 1, pp. 657–660, Mar. 2001, doi: 10.1109/77.919430.

[6] J. E. Lenz, "A review of magnetic sensors," *Proc. IEEE*, vol. 78, no. 6, pp. 973–989, Jun. 1990, doi: 10.1109/5.56910.

[7] J. Lenz and A. S. Edelstein, "Magnetic sensors and their applications," *IEEE Sensors J.*, vol. 6, no. 3, pp. 631–649, Jun. 2006, doi: 10.1109/JSEN.2006.874493.

[8] P. Ripka and M. Janosek, "Advances in magnetic field sensors," *IEEE Sensors J.*, vol. 10, no. 6, pp. 1108–1116, Jun. 2010, doi: 10.1109/JSEN.2010.2043429.

[9] W. Eerenstein, N. D. Mathur, and J. F. Scott, "Multiferroic and magnetoelectric materials," *Nature*, vol. 442, pp. 759–765, Aug. 2006, doi: 10.1038/nature05023.

[10] C. W. Nan, M. Li, and J. H. Huang, "Calculations of giant magnetoelectric effects in ferroic composites of rare-earth–iron alloys and ferroelectric polymers," *Phys. Rev. B, Condens. Matter*, vol. 63, no. 14, p. 144415, 2001, doi: 10.1103/PhysRevB.63.144415.

[11] J. Ryu, S. Priya, K. Uchino, and H. E. Kim, "Magnetoelectric effect in composites of magnetostrictive and piezoelectric materials," *J. Electroceramics*, vol. 8, pp. 107–119, 2002, doi: 10.1023/A:1020599728432.

[12] S. N. Babu, A. Siddeshwar, K. Srinivas, S. V. Suryanarayana, and T. Bhimasankaram, "Magnetoelectric properties of Ni/PZT/Ni layered composite for low field applications," *J. Mater. Sci.*, vol. 44, no. 15, pp. 3948–3951, 2009, doi: 10.1007/s10853-009-3534-4.

[13] K. H. Lam, C. Y. Lo, J. Y. Dai, H. L. W. Chan, and H. S. Luo, "Enhanced magnetoelectric effect in a stress-biased lead magnesium niobate-lead titanate single crystal/Terfenol-D alloy magnetoelectric sensor," *J. Appl. Phys.*, vol. 109, no. 2, p. 024505, 2011, doi: 10.1063/1.3536636.

[14] M. A. Ahmed, S. T. Bishay, and S. I. El-dek, "Magnetoelectric characteristics of $Dy_{2.8}Sr_{0.2}Fe_5O_{12}$ garnet (DySrIG)," *Eur. Phys. J.-Appl. Phys.*, vol. 59, no. 2, p. 20401, 2012, doi: 10.1051/epjap/2012110465.

[15] R. Jahns, A. Piorra, E. Lage, C. Kirchhof, D. Meyners, J. L. Gugat, M. Krantz, M. Gerken, R. Knöchel, and E. Quandt, "Giant magnetoelectric effect in thin-film composites," *J. Amer. Ceram. Soc.*, vol. 96, no. 6, pp. 1673–1681, Jun. 2013, doi: 10.1111/jace.12400.

[16] R. Ade, V. Sambasiva, J. Kolte, T. Karthik, A. R. Kulkarni, and N. Venkataramani, "Enhanced magnetoelectric response in 2-2 bilayer $0.50Pb(Ni_{1/3}Nb_{2/3})O_3$–$0.35PbTiO_3$–$0.15PbZrO_3/NiFe_2O_4$ thin films," *J. Phys. D, Appl. Phys.*, vol. 51, no. 11, p. 114004, 2018, doi: 10.1088/1361-6463/aaa98f.

[17] P. Martins, X. Moya, L. C. Phillips, S. Kar-Narayan, N. D. Mathur, and S. Lanceros-Mendez, "Linear anhysteretic direct magnetoelectric effect in $Ni_{0.5}Zn_{0.5}Fe_2O_4$/poly(vinylidene fluoride-trifluoroethylene) 0-3 nanocomposites," *J. Phys. D, Appl. Phys.*, vol. 44, no. 48, p. 482001, 2011, doi: 10.1088/0022-3727/44/48/482001.

[18] R. Gonçalves, A. Larrea, M. S. Sebastian, V. Sebastian, P. Martins, and S. Lanceros-Mendez, "Synthesis and size dependent magnetostrictive response of ferrite nanoparticles and their application in magnetoelectric polymer-based multiferroic sensors," *J. Mater. Chem. C*, vol. 4, no. 45, pp. 10701–10706, 2016, doi: 10.1039/c6tc04188d.

[19] J. Jin, F. Zhao, K. Han, M. Haque, L. Dong, and Q. Wang, "Multiferroic polymer laminate composites exhibiting high magnetoelectric response induced by hydrogen-bonding interactions," *Adv. Funct. Mater.*, vol. 24, no. 8, pp. 1067–1073, 2014, doi: 10.1002/adfm.201301675.

[20] L. Y. Fetisov, V. N. Serov, D. V. Chashin, S. A. Makovkin, G. Srinivasan, D. Viehland, and Y. K. Fetisov, "A magnetoelectric sensor of threshold DC magnetic fields," *J. Appl. Phys.*, vol. 121, no. 15, p. 154503, 2017, doi: 10.1063/1.4981533.

[21] V. Annapureddy, H. Palneedi, W.-H. Yoon, D.-S. Park, J.-J. Choi, B.-D. Hahn, C.-W. Ahn, J.-W. Kim, D.-Y. Jeong, and J. Ryu, "A pT/$\sqrt{\text{Hz}}$ sensitivity ac magnetic field sensor based on magnetoelectric composites using low-loss piezoelectric single crystals," *Sens. Actuators A, Phys.*, vol. 260, pp. 206–211, Jun. 2017, doi: 10.1016/j.sna.2017.04.017.

[22] Z. Y. Wu, L. X. Bian, S. X. Wang, and X. Y. Zhang, "An angle sensor based on magnetoelectric effect," *Sens. Actuators A, Phys.*, vol. 262, pp. 108–113, Aug. 2017, doi: 10.1016/j.sna.2017.04.049.

[23] Y. Wang, D. Gray, D. Berry, J. Gao, M. Li, J. Li, and D. Viehland, "An extremely low equivalent magnetic noise magnetoelectric sensor," *Adv. Mater.*, vol. 23, no. 35, pp. 4111–4114, 2011, doi: 10.1002/adma.201100773.

[24] Z. Chu, H. Shi, W. Shi, G. Liu, J. Wu, J. Yang, and S. Dong, "Enhanced resonance magnetoelectric coupling in (1-1) connectivity composites," *Adv. Mater.*, vol. 29, no. 19, p. 1606022, 2017, doi: 10.1002/adma.201606022.

[25] E. Quandt, S. Stein, and M. Wuttig, "Magnetic vector field sensor using magnetoelectric thin-film composites," *IEEE Trans. Magn.*, vol. 41, no. 10, pp. 3667–3669, Oct. 2005, doi: 0.1109/TMAG.2005.854793.

[26] S. Marauska, R. Jahns, H. Greve, E. Quandt, R. Knöchel, and B. Wagner, "MEMS magnetic field sensor based on magnetoelectric composites," *J. Micromech. Microeng.*, vol. 22, no. 6, p. 065024, 2012, doi: 10.1088/0960-1317/22/6/065024.

[27] S. Zare, J. Rabinowitz, H. Izadkhah, S. Somu, and C. Vittoria, "Magnetoelectric sensor excitations in hexaferrite films," *Appl. Phys. Lett.*, vol. 106, no. 19, p. 193502, 2015, doi: 10.1063/1.4921079.

[28] S. Salzer, V. Röbisch, M. Klug, P. Durdaut, J. McCord, D. Meyners, J. Reermann, M. Hoft, and R. Knochel, "Noise limits in thin-film magnetoelectric sensors with magnetic frequency conversion," *IEEE Sensors J.*, vol. 18, no. 2, pp. 596–604, Jan. 2018, doi: 10.1109/JSEN.2017.2776039.

[29] S. Reis, M. P. Silva, N. Castro, V. Correia, J. Gutierrez, A. Lasheras, and P. Martins, "Optimized anisotropic magnetoelectric response of $Fe_{61.6}Co_{16.4}Si_{10.8}B_{11.2}$/PVDF/$Fe_{61.6}Co_{16.4}Si_{10.8}B_{11.2}$ laminates for AC/DC magnetic field sensing," *Smart Mater. Struct.*, vol. 25, no. 5, p. 055050, 2016, doi: 10.1088/0964-1726/25/5/055050.

[30] Y. Long, J. Qiu, X. He, Q. Chang, Z. Hu, and H. Liu, "Flexible magnetoelectric transducer with high magnetic field sensitivity based on Metglas/poly(vinylidene fluoride) heterostructures," *Aip Adv.*, vol. 7, no. 12, p. 125029, 2017, doi: 10.1063/1.5013235.

[31] S. X. Dong, J. Zhai, J. Li, and D. Viehland, "Small DC magnetic field response of magnetoelectric laminate composites," *Appl. Phys. Lett.*, vol. 88, no. 8, p. 082907, 2006, doi: 10.1063/1.2178582.

[32] M. Silva, S. Reis, C. S. Lehmann, P. Martins, S. Lanceros-Mendez, A. Lasheras, J. Gutierrez, and J. M. Barandiaran, "Optimization of the magnetoelectric response of poly(vinylidene fluoride)/epoxy/vitrovac laminates," *ACS Appl. Mater. Interfaces*, vol. 5, no. 21, pp. 10912–10919, 2013, doi: 10.1021/am4031054.

[33] M. Li, D. Berry, J. Das, D. Gray, J. Li, and D. Viehland, "Enhanced sensitivity and reduced noise floor in magnetoelectric laminate sensors by an improved lamination process," *J. Amer. Ceram. Soc.*, vol. 94, no. 11, pp. 3738–3741, 2011, doi: 10.1111/j.1551-2916.2011.04659.x.

[34] J. Gao, D. Gray, Y. Shen, J. Li, and D. Viehland, "Enhanced dc magnetic field sensitivity by improved flux concentration in magnetoelectric laminates," *Appl. Phys. Lett.*, vol. 99, no. 15, p. 153502, 2011, doi: 10.1063/1.3650713.

[35] L. Shen, M. Li, J. Gao, Y. Shen, J. F. Li, D. Viehland, X. Zhuang, M. L. C. Sing, C. Cordier, S. Saez, and C. Dolabdjian, "Magnetoelectric nonlinearity in magnetoelectric laminate sensors," *J. Appl. Phys.*, vol. 110, no. 11, p. 114510, 2011, doi: 10.1063/1.3665130.

[36] S. Reis, M. P. Silva, N. Castro, V. Correia, P. Martins, A. Lasheras, J. Gutierrez, J. M. Barandiarán, J. G. Rocha, and S. Lanceros-Mendez, "Characterization of Metglas/poly(vinylidene fluoride)/Metglas magnetoelectric laminates for AC/DC magnetic sensor applications," *Mater. Des.*, vol. 92, pp. 906–910, Feb. 2016, doi: 10.1016/j.matdes.2015.12.086.

[37] F. N. Hooge, "1/f noise sources," *IEEE Trans. Electron Devices*, vol. 41, no. 11, pp. 1926–1935, Nov. 1994, doi: 10.1109/16.333808.

[38] P. Ripka, "Advances in fluxgate sensors," *Sens. Actuators A, Phys.*, vol. 106, nos. 1–3, pp. 8–14, 2003, doi: 10.1016/S0924-4247(03)00094-3.

[39] J. Tao, Y. Jia, H. Wu, and J. Yang, "Low-frequency nanotesla resolution of magnetic field detection in Metglas/magnetostrictive/piezoelectric laminates," *Adv. Materials Res.*, vols. 960–961, pp. 695–699, Jun. 2014, doi: 10.4028/www.scientific.net/AMR.960-961.695.

[40] S. Reis, N. Castro, M. P. Silva, V. Correia, J. G. Rocha, P. Martins, and S. Lanceros-Mendez, "Fabrication and characterization of high-performance polymer-based magnetoelectric DC magnetic field sensors devices," *IEEE Trans. Ind. Electron.*, vol. 64, no. 6, pp. 4928–4934, Jun. 2017, doi: 10.1109/TIE.2017.2668989.